Journal of Pharmacy and Pharmacology, 2023, **75**, 245–252
https://doi.org/10.1093/jpp/rgac085
Advance access publication 1 December 2022
Research Paper

JPP Journal of Pharmacy and Pharmacology

OXFORD

The manufacturing of 3D-printed microfluidic chips to analyse the effect upon particle size during the synthesis of lipid nanoparticles

Edward Weaver[1], Essyrose Mathew[1], Jay Caldwell[1], Andrew Hooker[2], Shahid Uddin[2] and Dimitrios A. Lamprou[1,*]

[1]School of Pharmacy, Queen's University Belfast, Belfast, UK,
[2]Immunocore Ltd, Milton Park, Abingdon, UK

[*]Correspondence: Dimitrios A. Lamprou, School of Pharmacy, Queen's University Belfast, 97 Lisburn Road, Belfast, BT9 7BL, UK. Email: D.Lamprou@qub.ac.uk

Abstract

Objectives The process of 3D printing to produce microfluidic chips is becoming commonplace, due to its quality, versatility and newfound availability. In this study, a UV liquid crystal display (LCD) printer has been implemented to produce a progression of microfluidic chips for the purpose of liposomal synthesis. The emphasis of this research is to test the limitations of UV LCD printing in terms of resolution and print speed optimisation for the production of microfluidic chips.

Key findings By varying individual channel parameters such as channel length and internal geometries, the essential channel properties for optimal liposomal formulation are being investigated to act as a basis for future experimentation including the encapsulation of active pharmaceutical ingredients. Using the uniquely designed chips, liposomes of ≈120 nm, with polydispersity index values of ≤0.12 are able to be reproducibly synthesised.

Conclusions The influence of total flow rates and lipid choice is investigated in depth, to provide further clarification on how a microfluidic setup should be optimised. In-depth explanations of the importance of each channel parameter are also explained throughout, with reference to their importance for the properties of a successful liposome.

Keywords: 3D Printing; microfluidics; liquid crystal display; liposomes; formulation

Introduction

The field of additive manufacturing (AM), also known as 3D printing (3DP), has evolved to a level whereby its influence is being felt throughout various related pharmaceutical fields, including microneedles,[1] tabletting[2] and, most poignantly for this study, microfluidics (MFs). Since its first successful application in 1983 by Charles W Hull using stereolithography (SLA),[3] the scope, accessibility and quality of AM have improved to facilitate its inception as an emerging technology within the healthcare sector. Various printer technologies have been developed to allow compatibility for a diverse range of materials, extending from thermoplastics, ceramics to edible materials.[4]

Liquid crystal display (LCD) printing technology shares similarities with SLA and digital light processing (DLP). Precise ultraviolet (UV) rays cause the solidification of liquid media, often resins, in a layer-by-layer approach. The cost-effective resolution possible from LCD is one of the most attractive features of the technology,[5] as well as the fact that its proficiency can progress in tandem with the development of LCD-based visual displays.[6] A schematic for LCD printing can be seen in Figure 1. Complex microstructures are able to be printed using LCD technology at a relatively cheap cost, making LCD printing a desirable process for future development. Both LCD and DLP printing allow for faster printing times as compared with SLA.[7] The limitations of the technology apply to most photo-curing methods, in that the spectrum of compatible materials can be limited.[6] Despite this fact, the resin used in this study offers high tensile strength and low shrinkage, both of which are essential for production and application for MF purposes.

The application of LCD printing for the fabrication of MF chips has sparsely been researched despite promising initial results. Most notably for the synthesis of liposomes, Ballacchino et al. produced multiple designs using both LCD and DLP printing and concluded that the designs allowed for the production of liposomes of equivalent quality to those produced using commercially obtained chips.[7] It is accepted that MF channel architectural parameters have a large effect on the formulation produced from the lab-on-a-chip device, which is why a plethora of designs are trialled in this research. The conjunction of this research with AM allowed for multiple designs to be produced within a limited amount of time. To discern the importance of individual parameters, such as channel length or mixing angle, a methodical approach of altering one parameter at a time was chosen. This study was an opportunity to test the limitations of LCD printing in terms of its resolution, special geometric functionality, material efficiency and speed. LCD printing was chosen over other forms of AM for a few main

Received: August 24, 2022. Editorial Acceptance: October 26, 2022

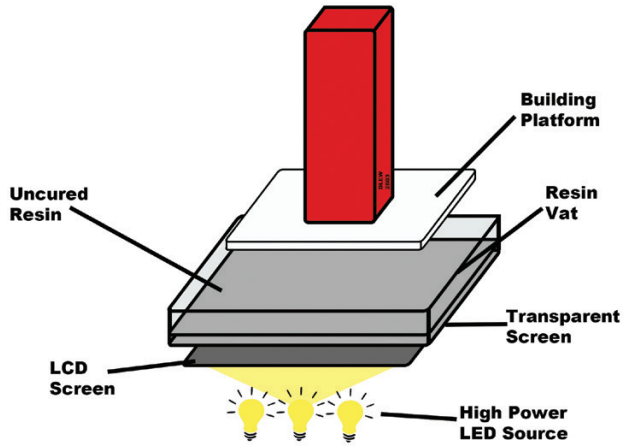

Figure 1 Essential components of LCD 3D printing technology.

reasons: the printing material of resin has been shown previously to be compatible with liposomal excipients and various APIs,[7, 8] the speed of LCD printing and the future potential of the technology.[9] Both fused deposition modelling and inkjet printing have been used previously to manufacture microfluidic chips, although there have been issues with these technologies such as extensive printing times or extensive post-processing.[10]

When producing liposomes via MFs, the phenomenon of self-assembly is relied upon for synthesis. Specific hydrophobic-hydrophilic interactions between phospholipids cause liposomal formation, which can be achieved via various methods. Traditional methods such as thin-film hydration (TFH) or sonication have been widely studied for liposomal synthesis, but they possess undesirable features including a lack of size control or excessive solvent use.[11] MFs, an emerging technology, provides an opportunity to improve both these features by combining reagents in a constricted volumetric environment to produce high-quality formulations without the need for post-processing methods, e.g. extrusion. MF has also been seen to increase the encapsulation efficiency of active pharmaceutical ingredients (APIs), even for those that have previously been a challenge to encapsulate, including RNA and biologics.[12, 13] This is especially potent during current times with the innovation of the lipid nanoparticle vaccine delivery system devised to combat the COVID-19 pandemic.

While 'standard' MF chips, such as those consisting of two inlets and a single mixing channel, provide a respectable means for liposomal production, there is still room for improvements in terms of the chip design. Increasing the length of the channels or introducing micromixing regions has seen improvements in the size, shape and polydispersity index (PDI) of liposomes; although little research has been performed when combining these factors to conclude the individual importance of each MF asset.

The effect of flow rate ratio (FRR) has been witnessed to have a dramatic on nanoparticle characteristics produced via MFs, especially for those that rely upon self-assembly for completion. The passive advection of liquid phases alongside hydrophobic/hydrophilic interactions is attributable to the formation of liposomes for phospholipids.[14] As highlighted, this study aims to derive the optimal microfluidic chips to determine the optimal MF characteristics for liposomal size, PDI and zeta-potential, while aiming to pinpoint which individual channel properties affect each aspect.

Materials and methods

Materials

White/Ivory photopolymer resin was obtained from Zortrax and was printed using the Zortrax Inkspire LCD printer. 1,2-dipalmitoyl-sn-glycero-3-phosphatidylcholine (DPPC) and 1,2-dioleoyl-sn-glycero-3-phasphatidylcholine (DOPC) and cholesterol (Figure 2), were obtained from Tokyo chemical industries (Tokyo, Japan). Tablets of phosphate-buffered saline (PBS) (pH7.4) and ethanol ≥99.8% were obtained from Sigma-Aldrich (Steinheim, Germany).

Production of MF chips via LCD printing

Chips designs were made using online computer-aided design software (TinkerCAD, Autodesk, USA). All chips were made to a 65 × 54 × 10 mm dimension, with varying internal channel geometry. All chips were made with internal cylindrical channels of 1 mm diameter. The names of all designs can be found in Figure 3.

Design chihuahua had a 35-mm-long cylindrical internal channel and inlet channels angled at 30°. All other chip designs had inlet channels angled at 60° and varied according to channel length or the presence of altered internal geometries. The design pug consisted of a 35-mm-long channel. The design retriever had a channel length of 70 mm. The design dachshund had a longer channel length of 110 mm. Design ridgeback and spaniel had 110 cm channel length and varied in the presence of specific internal geometries. Design ridgeback had 2 mm triangular wedges, 4 micromixers were placed in each horizontal direction of channels in the chip, totalling 12 throughout the chip. Design spaniel has semicircular internal geometries that were 2 mm in width, also placed along the horizontal direction, again with a total of 12 throughout. Three replicates of each chip design were produced and tested. A closer depiction of the internal geometries can be viewed in Figure 4.

Designs were exported as.stl files and printed using an Inkspire LCD printer (Zortrax, Olsztyn, Poland). Files were uploaded to Z-suite slicing software and sliced for printing. Prints were created using 0.025 µm resolution and White Basic resin. After printing, the print was removed from the build platform and placed in a bath of isopropyl alcohol and sonicated using Ultrawave QS12 Ultrasonic Bath (Cardiff, UK) to remove excess uncured resin from the print. Prints were then left to dry at room temperature for 30 min. Pictures of the final completed chips can be seen in Figure 5.

Production of liposomes via microfluidics

The Dolomite MF system was used to prepare liposomes, which consisted of two separate pressure chambers and flow rate sensors (0.2–5 ml/min capacity). Lipid/cholesterol solutions were prepared at a total concentration of 1 mg/ml in ethanol (≥99.8%), using a 2:1 lipid:cholesterol ratio as previously established by Briuglia et al.[15] All solutions prepared were briefly sonicated to verify complete dissolution. The lipid solution was passed through one inlet of the MF chip while a PBS solution was passed through the other as the aqueous phase. The TFR was adjusted throughout the study, ranging from 2 to 6 ml/min, as this has been observed to

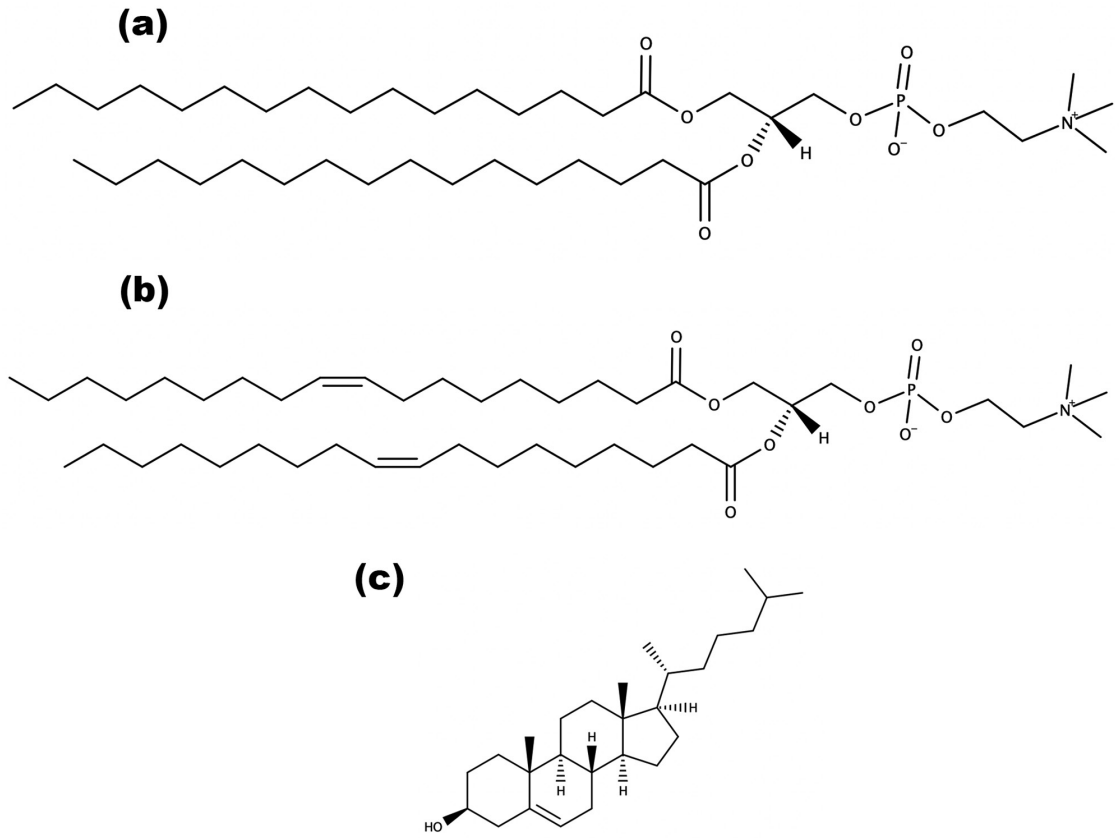

Figure 2 Chemical structures for (a) DPPC (hydrocarbon tail length n = 16), (b) DOPC (hydrocarbon tail length n = 18) and (c) cholesterol.

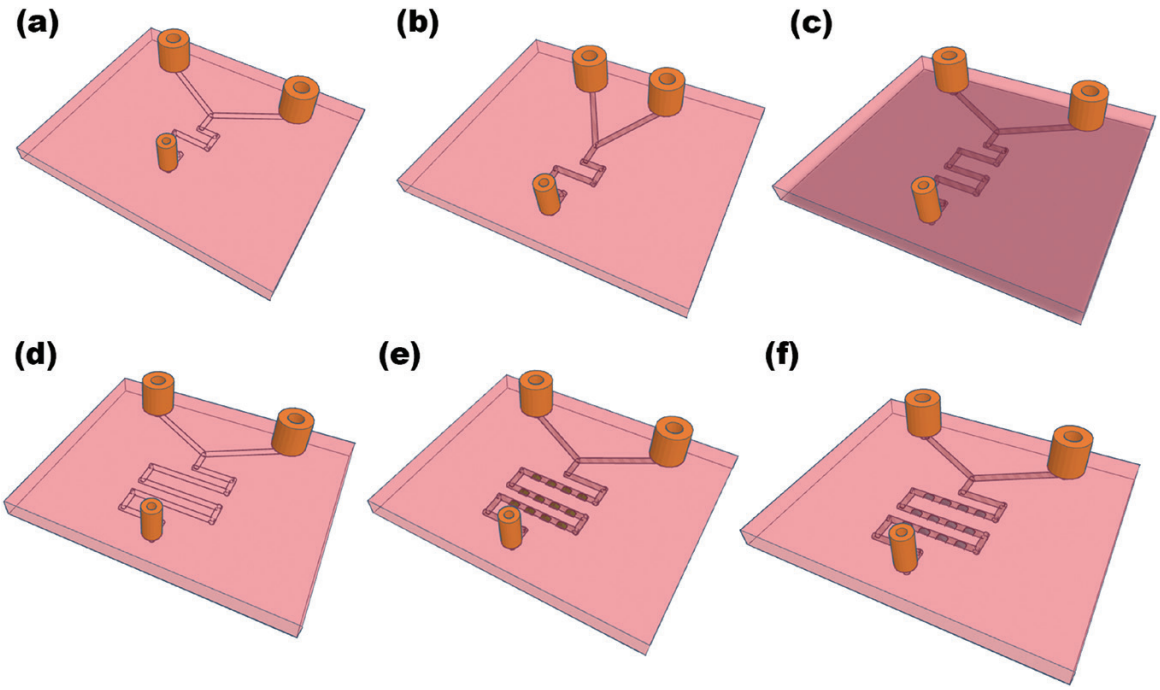

Figure 3 Schematics for the designs of the printed chips. Designs are named as followed: (a) pug, (b) chihuahua, (c) retriever, (d) dachshund, (e) ridgeback and (f) spaniel.

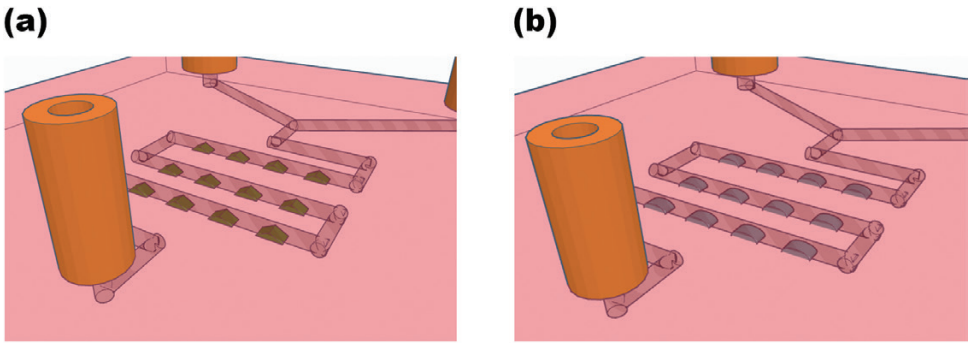

Figure 4 Internal channel geometries possessed by (a) design ridgeback and (b) design spaniel.

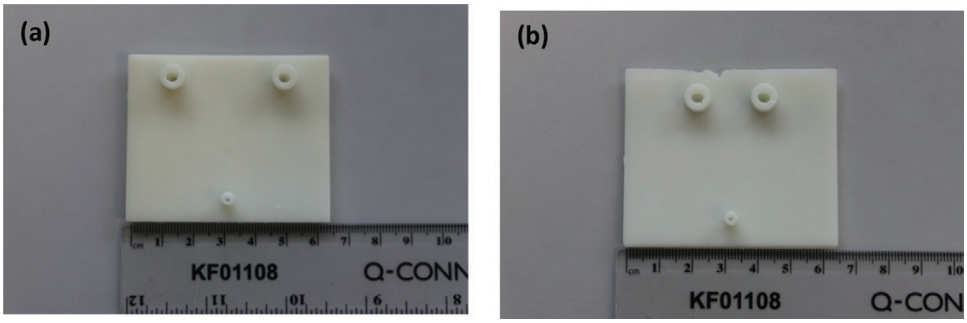

Figure 5 Pictures of (a) design pug and (b) design chihuahua. The internal capillaries of the MF chips are not visible due to the opaque nature of the resin used.

affect liposomal properties.[16] An FRR of 3:1 (Aqueous:Lipid) was maintained throughout, as it has been noted in various manuscripts to provide optimal liposomal qualities, such as size, stability and polydispersity.[17, 18]

Dynamic light scattering

Dynamic light scattering was employed to determine average particle size and PDI, using a Nanobrook Omni particle sizer (Brookhaven Instruments, Holtsville, NY, USA). Each measurement was performed in triplicate, using a 1-in-10 dilution with PBS. Zeta (ζ) potential was also measured with the Nanobrook Omni, measured in triplicate and averaged for result presentation. A total sample size of 2 ml was used for each assay, after dilution.

Statistical analysis

When required, data are presented as a mean value, coupled with a ±standard deviation. One-way ANOVA analysis was performed to determine statistical significance. For figures, * represents the significance of $P \leq 0.05$, and ** represents $P \leq 0.01$. The three main comparisons drawn for ANOVA were the difference between designs, the difference in TFRs and the difference between lipids.

Results and discussion

Design functionality

Despite multiple printing attempts and slight capillary modifications, the chihuahua design wouldn't allow the free passage of fluids through the capillaries. This is suggestive of limitations to the LCD printing process of producing capillaries at this specific angle. The channel post-mixing point was identified not to be the issue with this particular design, due to the design pug possessing exactly the same geometry post-mixing point. While LCD printing is a quick and economically efficient process, there are limitations associated with the technology, such as the resolution achievable, which is why design chihuahua was unable to effectively allow the complete passage of fluid. The current resolution available for LCD printing is stated to be 25 µm vertically and 50 µm on the XY axis, according to Zortrax. The narrower mixing angle used in the design chihuahua of 30° caused blockage of the channels.

It was observed that the printed chips were able to withstand total flow rates of up to 7 ml/min. Beyond this value, fluid began flowing in a bidirectional manner and caused inlets to rupture slightly due to the unsustainable pressure within the chip. It is theorised that the flow rate could be increased should the capillaries be widened beyond 1 mm, however, this would affect the size and PDI of liposomes produced.

Each chip produced was run for at least 2 min at a time to produce the sample at least nine times. The chips showed no sign of degradation or reduction in the quality of liposomes produced.

The use of the white/ivory resin prevented the visual characterisation of the internal capillaries; however, this resin was chosen due to its favourable mechanical properties upon printing as compared with other translucent/clear resins.

LCD printing is commonly accepted as a time-efficient form of 3DP as, despite still following the classic 'layer-by-layer' approach, the technology is capable of curing an entire layer simultaneously. As previously seen by Ballacchino et al., the printing speed as compared with alternative 3DP

techniques such as fused deposition modelling and SLA was decreased using UV LCD printing.[7] The average print time of the chips was 2 h and 2 min using the parameters chosen. Decreasing the print time makes the process more environmentally friendly and industrially viable.[19]

Liposomal results

Particle diameter

The size of a liposome is essential to monitor, as it will drastically affect the pharmacokinetic/pharmacodynamic properties possessed by a formulation. The liposomes produced in this study consisted of a vacant aqueous core; hence it isn't justifiable to determine which size would be optimal for a specific use. The benefit of producing liposomes of various sizes across the devices is that a specific device can be chosen depending on the size requirement of the formulation.

A one-way ANOVA analysis determined the existence of a statistical difference between the sizes produced across the devices. The main finding from comparing particle sizes between devices was that increasing the length of the channel within the MF device reduced the size of the particles produced, for both lipids. Increasing the length of the channel from 35 to 110 mm resulted in the reduction of particle size, owing to an increased duration of time available for the advection of liquid media within the channels.

The introduction of internal geometrical micromixers in designs ridgeback and spaniel reduced the effect of TFR upon the size of the liposomes, as can be seen in Figure 6. This effect can be derived back to studies performed on the laminar flow alterations that occur within the microchannels.[20] The flow speed observed through the MF chip is disrupted due to the micromixing regions. The overall particle size is reduced as compared with the devices without the altered internal geometries; however, there exists little difference in overall flow rates when injecting different TFRs.[20]

Initially, the DOPC lipid was chosen as a negative control to help draw a comparison between the self-assembly process that occurs upon MF mixing. In relation to MFs, DOPC has often produced poor quality due to its unsaturated nature and its relatively low thermal transition temperature.[17] The results displayed in designs ridgeback and spaniel, however, suggest that the presence of internal geometries within the spaniel device is more favourable for the formation of smaller liposomes

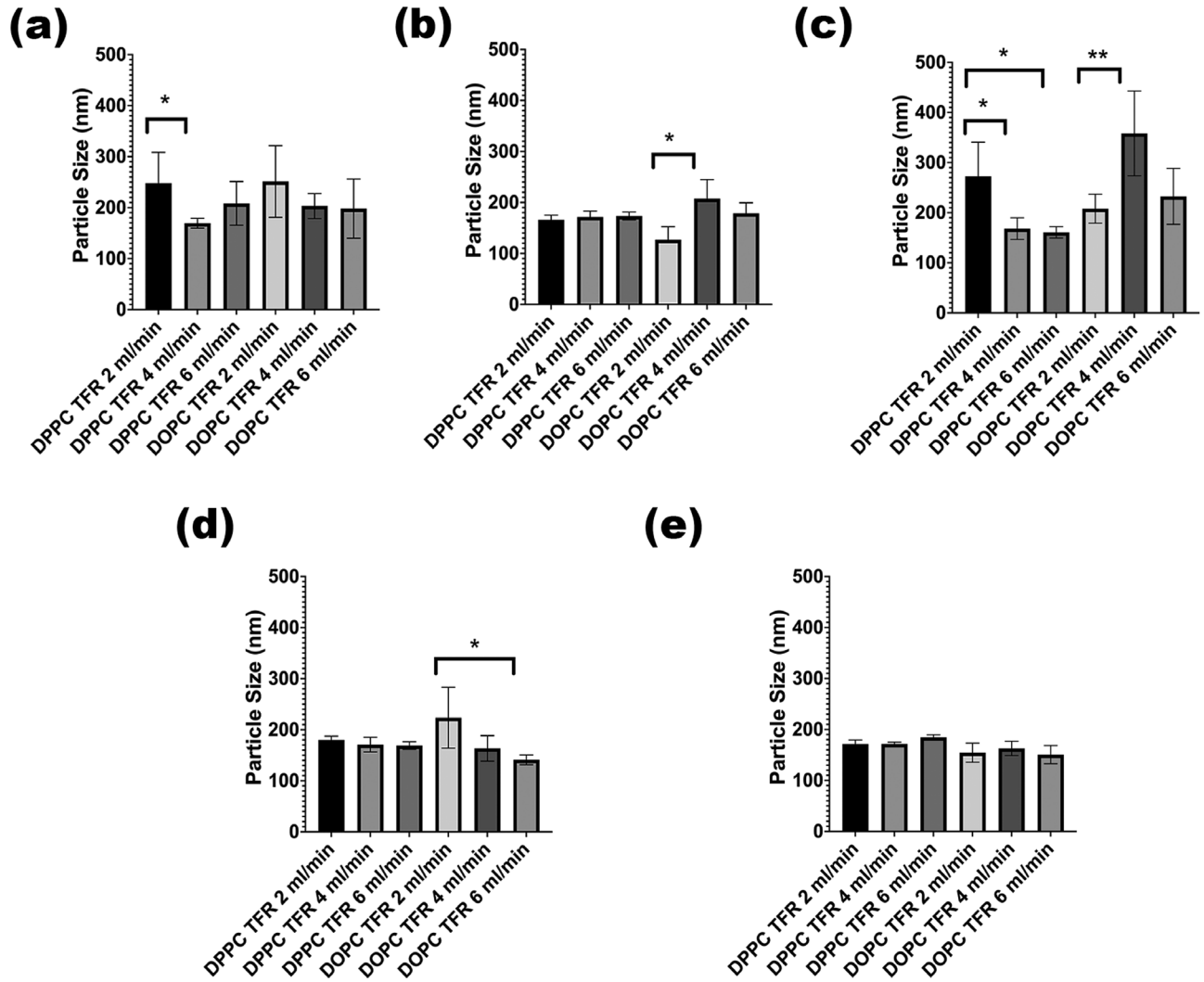

Figure 6 Particle size results for designs (a) pug, (b) retriever, (c) dachshund, (d) ridgeback and (e) spaniel MF chips. * represents the significance of $P \leq 0.05$, and ** represents $P \leq 0.01$.

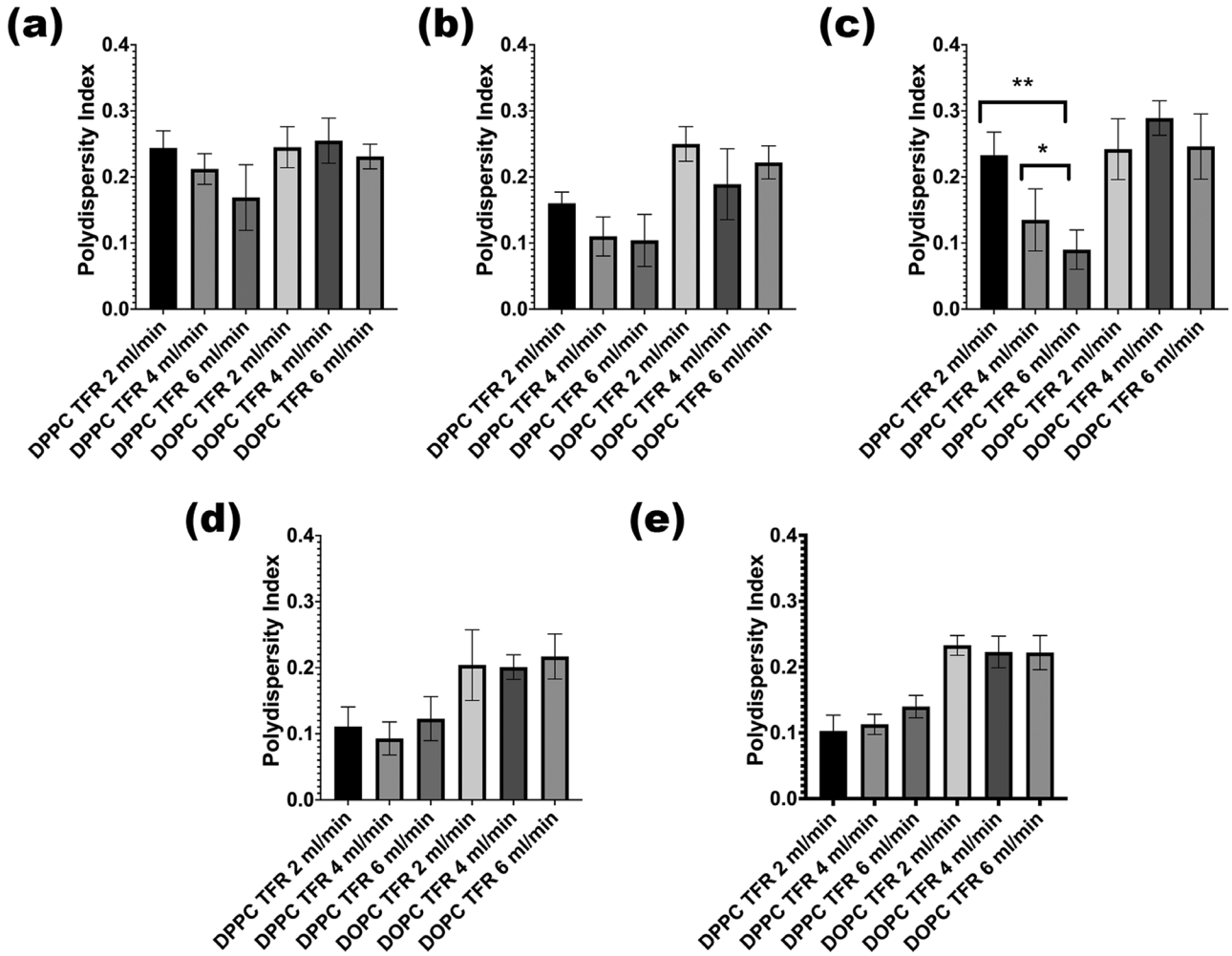

Figure 7 Polydispersity data obtained for designs (a) pug, (b) retriever, (c) dachshund, (d) ridgeback and (e) spaniel. * represents the significance of $P \leq 0.05$, and ** represents $P \leq 0.01$.

using DOPC. DOPC liposomes produced using these devices produce generally smaller liposomes than those of DPPC at the higher flow rate of 6 ml/min, although it should be noted the difference between the liposome sizes isn't statistically significant according to the ANOVA analysis. It's suggested from the beginning of this trend that the presence of micromixing regions within the capillaries may help overcome the physical limitations of the double bonds present in the DOPC, causing a more compact liposomal membrane to be formed.

As has been displayed in previous research, increasing the TFR causes the formation of liposomes with smaller diameters,[16, 21] although using the chip designs in this design, the effect isn't mathematically significant. The benefit however of using higher flow rates in the industry, especially if they produce slightly more optimal formulations, is the reduction in time for synthesis. Due to limitations posed by the system, and the desired FRR used, the TFR was limited to 6 ml/min, although if a similar trend is followed as proposed in the literature, especially beyond 10 ml/min, the particle size would be likely to reduce further.[21]

Polydispersity

In general, a formulation is considered to be monodisperse if the PDI lies below 0.2,[22] which is obtained for multiple of the formulations produced in this study when considering DPPC. MFs boasts the capacity to produce formulations with low PDI values without the requirement for post-processing. It was the goal of this particular study to identify channel attributes and MF parameters that allow for the production of liposomes with optimal polydispersity values.

The value of PDI within a nanoparticle formulation is often understated, although it is tied closely to important properties of a medicine, including the release profile, stability and pharmacokinetics (PKs). It's clear from the results of Figure 7 that DOPC produces less homogenous formulations via MFs than DPPC, which is attributable to the unsaturated nature of the lipid.[17] The ANOVA analysis confirms this, establishing a statistically significant difference in PDI between the two lipids when comparing all devices. DPPC formulations, as suspected from previously seen data follow a trend of having well-controlled PDI when using MFs.

It's clear that the presence of micromixing regions within the channels contributes towards the production of reproducible formulations with low PDI values, as displayed by designs ridgeback and spaniel.

The general trend in the literature shows that increasing the TFR used within an MF system allows for smaller particles to

Table 1 Zeta potential results obtained for all chip designs. Data presented represent an average of three replicated, presented with a ±SD

Design	Zeta potential (mV)											
	DPPC						DOPC					
	TFR 2 ml/min	SD	TFR 4 ml/min	SD	TFR 6 ml/min	SD	TFR 2 ml/min	SD	TFR 4 ml/min	SD	TFR 6 ml/min	SD
Pug	−7.79	1.13	−7.45	2.41	−6.11	1.05	−10.32	1.05	−9.02	2.42	−11.82	2.44
Chihuahua	−5.68	3.08	−6.67	1.37	−4.28	2.22	−8.03	2.44	−5.49	1.82	−6.30	2.09
Dachshund	−10.33	2.10	−12.58	1.75	−11.47	2.08	−10.09	1.85	−9.35	1.47	−10.71	2.37
Ridgeback	−5.78	0.96	−7.01	0.81	−5.92	1.80	−4.55	0.95	−5.39	1.11	−5.43	1.48
Spaniel	−8.00	1.52	−5.74	0.57	−6.15	1.43	−5.98	0.46	−4.98	1.10	−5.15	1.02

be produced, but at the sacrifice of increasing the PDI.[18, 23] This trend is caused by increasing the kinetic energy within the MF channels, in turn increasing the entropy at which liposomes are formed.[24] This trend isn't followed for designs pug, retriever and dachshund. This is likely due to the relatively high width of channels produced in comparison to commercial chips, which negates slightly the effect of TFR upon controlling the PDI of the formulation.[25]

When considering the PDI values produced for DPPC liposomes across all samples, excluding pug TFR 2 ml/min and dachshund TFR 2 ml/min, all formulations could be deemed homogenous. This suggests that the printed chips are highly functional for liposomal preparation.

Zeta (ζ) potential

Both isolated DPPC and DOPC are considered to be more neutral lipids in comparison with lipids such as commercially available phosphatidylcholine (PC) (consisting of a mixture of various PCs), however, the analysis of ζ-potential is essential for the prediction of aspects of a formulation such as encapsulation efficiency, formulation stability and PKs.

The data presented demonstrate the fact that altering the design of the chip affects the ζ-potential of the formulation, due to a slightly altered chemical composition of the liposomes between devices. There is an established linear relationship between ζ-potential and the percentage molar ratio of charged lipids in a liposome.[26] The lipid/cholesterol concentration and FRR remained constant throughout the experiments, meaning that a change in ζ-potential derives from a different self-assembly order taking place between devices, altering the composition of the liposomes formed.

This fact is further backed up by the fact that the TFR doesn't have a statistically significant effect on ζ-potential, as seen in Table 1. The size of a particle is linked loosely to the ζ-potential of a formulation,[27] which will account slightly for the altering ζ-potential, due to changing surface area to volume ratios.

Anionic lipid carriers such as the two used in this study appear as strong candidates for the encapsulation of cationic APIs due to favourable electrostatic interactions, as has also been previously in the literature.[28] Processes that rely solely upon the passive encapsulation of APIs, including TFH, often struggle to encapsulate anionic APIs, e.g. DNA/RNA. MFs enforces the concept of encapsulation via volumetric restriction due to a controlled active mixing process. It's predicted that designs ridgeback and spaniel would allow for increased encapsulation due to the presence of additional mixing regions within the encapsulation process.

Conclusions

The suggested designs, apart from the Chihuahua, all functioned as MF devices to produce liposomes, both monodisperse (PDI < 0.2) and polydisperse (PDI > 0.2) over a spectrum of particle sizes. When considering specifically the monodisperse formulations, the optimised chips also produced a narrow scope of particle sizes, allowing the technology to be a practical means of reproducible liposomal synthesis. It was clear to see that altering the geometrical properties of the channels had an effect on liposomal properties, especially with the introduction of internal channel geometries as possessed by designs ridgeback and spaniel. Increasing the length of channels showed a correlation with the production of smaller liposomes with more controlled PDIs. This research has highlighted which elements of an MF chip are essential to improve the physicochemical properties of a liposome, while providing indications of which designs may be more suitable for use during API encapsulation. There was no clear difference between the efficacies of triangular or semicircular micromixers within the channels, however, their presence did ameliorate the quality of the liposomes produced.

In summary for the channel properties, the optimal chip designs possessed a longer channel length to allow for increased mixing times, coupled with micromixing regions to decrease both the size and PDI of the formulation. LCD printing is an acceptable method for the production of MF chips with various properties in a timely and cost-efficient manner, although there are still areas that the technology must develop in to allow for further progress, such as increasing the resolution capacity.

Authors Contributions

Conceptualisation, D.A.L. and E.W.; methodology, E.W, E.M and J.C.; software, J.C.; validation, D.A.L., E.W., E.M. and J.C..; formal analysis, E.W. and J.C.; investigation, E.W., E.M. and J.C.; resources, S.U. and D.A.L.; data curation, E.W., E.M. and J.C.; writing—original draft preparation, E.W. and E.M.; writing—review and editing, D.A.L., S.U., A.H., E.W., E.M. and J.C.; visualisation, E.W.; supervision, D.A.L.; funding acquisition, S.U., A.H. and D.A.L. All

authors have read and agreed to the published version of the manuscript.

Funding

This research was funded by Immunocore.

Conflict of Interest

S.U. and A.H. are employees of Immunocore. All authors declare no conflict of interest.

Data availability

Data available on request due to restrictions, e.g. privacy or ethical.

References

1. Mathew E, Pitzanti G, Gomes Dos Santos AL et al. Optimization of printing parameters for digital light processing 3d printing of hollow microneedle arrays. *Pharmaceutics* 2021; 13: 1837. https://doi.org/10.3390/pharmaceutics13111837
2. Chen G, Xu Y, Chi Lip Kwok P et al. Pharmaceutical applications of 3d printing. *Addit Manuf* 2020; 34: 101209. https://doi.org/10.1016/j.addma.2020.101209
3. Hull CW. The birth of 3D printing. *Res Technol Manage* 2015; 58: 25–30.
4. Feng C, Zhang M, Bhandari B. Materials properties of printable edible inks and printing parameters optimization during 3D printing: a review. *Crit Rev Food Sci Nutr* 2019; 59: 3074–81. https://doi.org/10.1080/10408398.2018.1481823
5. Xenikakis I, Tsongas K, Tzimtzimis EK et al. Fabrication of hollow microneedles using liquid crystal display (LCD) vat polymerization 3D printing technology for transdermal macromolecular delivery. *Int J Pharm* 2021; 597: 120303. https://doi.org/10.1016/j.ijpharm.2021.120303
6. Quan H, Zhang T, Xu H et al. Photo-curing 3D printing technique and its challenges. *Bioact Mater* 2020; 5: 110–5. https://doi.org/10.1016/j.bioactmat.2019.12.003
7. Ballacchino G, Weaver E, Mathew E et al. Manufacturing of 3D-printed microfluidic devices for the synthesis of drug-loaded liposomal formulations. *Int J Mol Sci* 2021; 22: 8064. https://doi.org/10.3390/ijms22158064
8. Chen Z, Han JY, Shumate L et al. High throughput nanoliposome formation using 3D printed microfluidic flow focusing chips. *Adv Mater Technol* 2019; 4: 1800511. https://doi.org/10.1002/admt.201800511
9. Xu X, Seijo-Rabina A, Awad A et al. Smartphone-enabled 3D printing of medicines. *Int J Pharm* 2021; 609: 121199. https://doi.org/10.1016/j.ijpharm.2021.121199
10. Weisgrab G, Ovsianikov A, Costa PF. Functional 3D printing for microfluidic chips. *Adv Mater Technol* 2019; 4: 1900275. https://doi.org/10.1002/admt.201900275
11. Zhang, H., Thin-film hydration followed by extrusion method for liposome preparation. In: D'Souza G (ed.), *Liposomes*. Methods in Molecular Biology, Vol. 1522. New York, NY: Humana Press, 2017. https://doi.org/10.1007/978-1-4939-6591-5_2.
12. Weaver E, Uddin S, Cole DK et al. The present and future role of microfluidics for protein and peptide-based therapeutics and diagnostics. *Appl Sci* 2021; 11: 4109. https://doi.org/10.3390/app11094109
13. Maeki M, Uno S, Niwa A et al. Microfluidic technologies and devices for lipid nanoparticle-based RNA delivery. *J Control Release* 2022; 344: 80–96.
14. Ran R, Wang H, Liu Y et al. Microfluidic self-assembly of a combinatorial library of single-and dual-ligand liposomes for in vitro and in vivo tumor targeting. *Eur J Pharm Biopharm* 2018; 130: 1–10. https://doi.org/10.1016/j.ejpb.2018.06.017
15. Briuglia M-L, Rotella C, McFarlane A et al. Influence of cholesterol on liposome stability and on in vitro drug release. *Drug Deliv Transl Res* 2015; 5: 231–42. https://doi.org/10.1007/s13346-015-0220-8
16. Aghaei H, Solaimany Nazar AR. Continuous production of the nanoscale liposome in a double flow-focusing microfluidic device. *Ind Eng Chem Res* 2019; 58: 23032–45.
17. Weaver E, O'Connor E, Cole DK et al. Microfluidic-mediated self-assembly of phospholipids for the delivery of biologic molecules. *Int J Pharm* 2022; 611: 121347. https://doi.org/10.1016/j.ijpharm.2021.121347
18. Forbes N, Hussain MT, Briuglia ML et al. Rapid and scale-independent microfluidic manufacture of liposomes entrapping protein incorporating in-line purification and at-line size monitoring. *Int J Pharm* 2019; 556: 68–81. https://doi.org/10.1016/j.ijpharm.2018.11.060
19. Weaver E, O'Hagan C, Lamprou DA. The sustainability of emerging technologies for use in pharmaceutical manufacturing. *Expert Opin Drug Deliv* 2022; 19: 861–72. https://doi.org/10.1080/17425247.2022.2093857
20. Shi H, Zhao Y, Liu Z. Numerical investigation of the secondary flow effect of lateral structure of micromixing channel on laminar flow. *Sens Actuators B* 2020; 321: 128503.
21. Sedighi M, Sieber S, Rahimi F et al. Rapid optimization of liposome characteristics using a combined microfluidics and design-of-experiment approach. *Drug Deliv Transl Res* 2019; 9: 404–13. https://doi.org/10.1007/s13346-018-0587-4
22. Shamarekh KS, Gad HA, Soliman ME, Sammour OA. Towards the production of monodisperse gelatin nanoparticles by modified one step desolvation technique. *J Pharm Investig* 2020; 50: 189–200.
23. Roces CB, Lou G, Jain N et al. Manufacturing considerations for the development of lipid nanoparticles using microfluidics. *Pharmaceutics* 2020; 12: 1095. https://doi.org/10.3390/pharmaceutics12111095
24. Chiesa E, Greco A, Riva F et al. Staggered herringbone microfluid device for the manufacturing of chitosan/TPP nanoparticles: systematic optimization and preliminary biological evaluation. *Int J Mol Sci* 2019; 20: 6212. https://doi.org/10.3390/ijms20246212
25. Michelon M, Oliveira DRB, de Figueiredo Furtado G et al. High-throughput continuous production of liposomes using hydrodynamic flow-focusing microfluidic devices. *Colloids Surf B* 2017; 156: 349–57. https://doi.org/10.1016/j.colsurfb.2017.05.033
26. Smith MC, Crist RM, Clogston JD et al. Zeta potential: a case study of cationic, anionic, and neutral liposomes. *Anal Bioanal Chem* 2017; 409: 5779–87. https://doi.org/10.1007/s00216-017-0527-z
27. Foteini P, Pippa N, Naziris N et al. Physicochemical study of the protein–liposome interactions: influence of liposome composition and concentration on protein binding. *J Liposome Res* 2019; 29: 313–21. https://doi.org/10.1080/08982104.2018.1468774
28. Dichello GA, Fukuda T, Maekawa T et al. Preparation of liposomes containing small gold nanoparticles using electrostatic interactions. *Eur J Pharm Sci* 2017; 105: 55–63. https://doi.org/10.1016/j.ejps.2017.05.001